The official journal of the Japan Atherosclerosis Society and
the Asian Pacific Society of Atherosclerosis and Vascular Diseases

Original Article

J Atheroscler Thromb, 2023; 30: 138-149. http://doi.org/10.5551/jat.63460

Elevated Fibroblast Growth Factor 23 Impairs Endothelial Function through the NF-κB Signaling Pathway

Li-wei Guo[1, 2], Yi-kai Wang[1, 2], Shi-jie Li[1, 2], Guo-tian Yin[3] and Duan Li[1]

[1]School of Forensic Medicine, Xinxiang Medical University, Henan, China.
[2]Xinxiang Key Laboratory of Metabolism and Integrative Physiology, Henan, China.
[3]The Third Affiliated Hospital of Xinxiang Medical University, Henan, China.

Aim: Roles of fibroblast growth factor 23 (FGF23) in endothelial dysfunction remain controversial, and evidence from population-based studies is lacking. The present study aimed to explore the effects of FGF23 on endothelial dysfunction on the basis of both clinical data of patients with coronary artery disease (CAD) and the *in vitro* research in human umbilical vein endothelial cells (HUVECs).

Methods: A total of 321 CAD patients were enrolled after coronary angiography, brachial artery flow-mediated dilation (FMD) was assessed using ultrasound equipment. Serum FGF23, nitric oxide (NO), and endothelin-1 (ET-1) were detected via enzyme-linked immunosorbent assay. Apoptosis was determined using the annexin V-fluorescein isothiocyanate/propidium lodide apoptosis detection kit. Cell migration was evaluated by wound healing and transwell migration assays. Reactive oxide species levels were determined using fluorescent probes, and NF-κB p65 nuclear translocation was assessed via immunofluorescence.

Results: Serum FGF23 was significantly increased in CAD patients combined with severe endothelial dysfunction (FMD <2%) compared to those with FMD ≥ 2% ($P<0.001$). Furthermore, the levels of FGF23 were negatively correlated with NO, whereas positively correlated with ET-1 both in unadjusted analysis and multivariate-adjusted analysis. In HUVECs, FGF23 interfered with the bioavailability of NO via increased oxidative stress. Moreover, FGF23 directly impaired the endothelium by promoting HUVECs apoptosis and attenuating the migration of HUVECs. Additional experiments showed that FGF23 induced endothelial injury through activation of the NF-κB signaling pathway.

Conclusions: Elevated FGF23 is clinically associated with endothelial dysfunction in CAD patients, and FGF23 impairs endothelial function through activation of the NF-κB signaling pathway.

Key words: Fibroblast growth factor 23, Endothelial dysfunction, NF-κB signaling pathway

Introduction

Endothelial dysfunction is recognized as an early event in the pathological process of atherosclerosis (AS) and is also the basis for the occurrence and deterioration of coronary artery disease (CAD)[1, 2]. Fibroblast growth factor 23 (FGF23) is secreted mainly by osteocytes and osteoblasts and regulates the homeostasis of calcium and phosphorus by interacting with its coreceptor Klotho[3]. Recent studies have shown that FGF23 is closely related to the occurrence and development of CAD[4, 5]. Evidence from epidemiological studies suggested that high levels of FGF23 can be used as a nontraditional risk factor for CAD[6], and functional studies also found that FGF23 may damage endothelial function in a direct or indirect way[7]. Nevertheless, the roles of FGF23 have recently been found to be more complex than previously thought. A major question that remains unresolved is whether FGF23 can directly act on

Address for correspondence: Duan Li, School of Forensic Medicine, Xinxiang Medical University, No. 601 Jinsui Road, Hongqi District, Xinxiang, 453003, Henan, China E-mail: 061014@xxmu.edu.cn

Received: December 19, 2021 Accepted for publication: February 21, 2022

endothelial cells to promote or inhibit endothelial dysfunction. Silswal *et al*[8] showed that FGF23 hindered nitric oxide (NO) bioavailability in the endothelium by stimulating the synthesis of superoxide anion; contrarily, Lindberg *et al*[9] failed to observe an FGF23 effect on aorta reactivity. Conversely, Richter *et al*[10] reported that Klotho modulated FGF23-mediated NO synthesis and oxidative stress in human coronary artery endothelial cells. Thus, to elucidate the specific mechanism of FGF23 participation in endothelial dysfunction, further research is still required.

In this study, we confirmed the correlation of FGF23 with endothelial dysfunction on the basis of clinical data of patients with CAD and from the *in vitro* basic research in human umbilical vein endothelial cells (HUVECs).

Methods

Materials

Recombinant human FGF23 was purchased from PeproTech.Inc (Rocky Hill, NJ, USA). NF-κB inhibitor BAY11-7082 was obtained from Beyotime (Shanghai, China). Fibroblast growth factor receptor (FGFR) inhibitor BGJ398 was obtained from Selleck Chemicals (Houston, TX, USA). Methylamino-2′,7′-difluorofluorescein diacetate (DAF-FM) and dihydroethidium (DHE) were obtained from Invitrogen (Carlsbad, CA, USA). Monoclonal antibodies against eNOS, p-eNOS (ser1177), p-eNOS(thr495), Cleaved-Caspase3, Caspase3, Bax, p65, p-p65, IκBα, and p-IκBα were acquired from Cell Signaling Technology (Beverly, MA, USA). Antibodies against Nox2, p47phox, p67phox, β-actin, and goat anti-rabbit IgG antibodies were from Wanleibio (Shenyang, China).

Study Subjects

A total of 321 patients with CAD were enrolled from The Third Affiliated Hospital of Xinxiang Medical University, including 189 males and 132 females, aged 40–78 years. All patients were confirmed via coronary angiography with at least 70% stenosis in a major epicardial artery or 50% stenosis in the left main coronary artery. Subjects with valvular heart disease, chronic kidney diseases, severe liver disease, cardiomyopathy, familial hypercholesterolemia, thyroid disease, malignant tumor, cognitive dysfunction, dementia, severe mental illness, history of trauma, and surgery within 3 months were excluded.

Informed consent was obtained from all subjects before inclusion in the study. This study conformed to the principles outlined in the Declaration of Helsinki and was approved by the Ethics Committee of Xinxiang Medical University.

Basic Investigation

General clinical information of all patients was collected and recorded, including age, gender, body mass index (BMI), smoking status, systolic blood pressure (SBP), diastolic blood pressure (DBP), history of smoking, history of medication, and family history. The peripheral blood was collected from all participants after fasting for 10 h and then centrifuged at 2000 r/min for 15 min; the serum was separated and stored at −80℃. Fasting blood glucose (FBG), total cholesterol (TC), triglyceride (TG), high-density lipoprotein–cholesterol (HDL–C), and low-density lipoprotein–cholesterol (LDL–C) were measured using Beckman AU5800 auto biochemistry analyzer (Beckman Coulter, CA, USA). Serum calcium and phosphorus were determined using the enzyme method.

Flow-Mediated Dilation Assessment

Flow-mediated dilation (FMD) of the brachial artery was conducted according to the American College of Cardiology guidelines[11]. The subjects rested in the supine position for 10–15 min before the test. Brachial artery ultrasound scans were performed using the Siemens ACUSON Sequoia 512 ultrasound machine (Berlin, Germany) with an 8.0-MHz transducer. A standard pediatric cuff was placed on the upper left arm to record BP at baseline and the end of the test. To create a flow stimulus, the cuff was inflated to the right forearm at least 50 mmHg above the baseline SBP (but did not exceed 200 mmHg) to occlude artery inflow for 5 min. At the end of 5 min of ischemia, brachial artery diameter was measured above the cuff within 1 min after releasing occlusion. FMD was calculated using the formula as follows: (maximum diameter − baseline diameter)/baseline diameter × 100%.

Patients were divided into tertiles according to their baseline FMD values: tertile 1 (< 2%, low FMD), tertile 2 (2%–7.1%, medium FMD), and tertile 3 (≥ 7.1%, high FMD). To classify the patients according to the severity of the endothelial dysfunction, we used the FMD cutoff value of the first tertile (< 2%, low values of FMD) to discriminate between those with severe endothelial dysfunction from the remaining patients with nonsevere endothelial dysfunction (≥ 2%, tertiles 2 and 3).

Serum FGF23, NO, and Endothelin-1 Assessment

Enzyme-linked immunosorbent assay method

was used to determine the levels of serum FGF23, NO, and endothelin-1 (ET-1). The relevant kits were purchased from Huamei Biological Engineering (Wuhan, China). The absorbance value of each well was measured at 450 nm using Thermo Scientific Multiskan FC (Waltham, MA, USA).

Cell Isolation and Culture

HUVECs were isolated from the human umbilical vein vascular wall by digestion with collagenase. Then, the cells were cultured in an endothelial cell culture medium with 10% fetal bovine serum (FBS), 1% endothelial cell growth supplement, 100 U/mL penicillin, and 100 mg/mL streptomycin sulfate at 37℃ in a humidified incubator with 5% CO_2. Cells from passages 3–8 were used for experiments.

Measurement of Intracellular NO Production

NO production by HUVECs was assessed using DAF-FM DA, a specific NO probe. After overnight serum starvation, HUVECs were incubated with vehicle or FGF23 for 24 h. Subsequently, cells were trypsinized and loaded with DAF-FM DA (10 μM) at 37℃ for 20 min in the dark, a population of 10,000 cells was gated and segregated on the basis of their relative fluorescence intensity using flow cytometry with the parameters of fluorescein isothiocyanate (FITC).

The total nitrate was determined by the Griess reagent. Absorbance was read at 540 nm after incubation of the mixture at 37℃ for 10 min, and the concentrations (μM) of total nitrate were calculated from a standard curve.

Measurement of Production of Reactive Oxygen Species (ROS)

HUVECs were treated with vehicle and FGF23 for 24 h followed by incubation with DHE (5 mM) solution at 37℃ for 30 min in the dark. Red fluorescence intensity was recorded using a fluorescence microscope with optimized excitation and emission wavelengths (DHE, 518/603 nm) at 20× magnification, the intensity of fluorescence was analyzed using Image-J software.

Apoptosis Assay

Cells were collected and detected using propyl iodide (PI)/annexin V-FITC apoptosis detection kit (BD Biosciences, USA). Annexin V-FITC and PI were added to the collected cells, then incubated in an incubator for 20 min in darkness. Cell apoptosis was assessed via flow cytometry and apoptosis rate was defined as the percentage of cells in the upper right quadrant and lower right quadrant.

Scratch Wound Healing Assay

HUVECs were laid on a six-well plate at 1.0×10^6 cells/well and grown to confluence; then, the cells were scratched by a straight line using sterile pipette tips. Afterward, the cells were cultured in a serum-free medium with vehicle or FGF23. Wound images at 24 h were obtained using an inverted microscope. The scratch area was measured by wound area and wound healing percentage using the Image-J software.

Transwell Cell Migration Assay

Before the experiment, the cells were starved in a serum-free medium for 6 h, then 1.0×10^5 HUVECs, in serum-free medium, were seeded into the upper chamber of a transwell insert (8-mm pore size, Corning Inc.), and a medium with 20% FBS was added in the lower chamber as a chemoattractant. After 24 h culture in 37℃ at the incubator, the medium and cells that did not migrate from the top of the membrane were removed. Then, after crystal violet staining, the upper chamber was observed under an electron microscope and counted the number of cells in different fields of view to get an average sum of cells that have migrated through the membrane toward the medium and attached to the underside of the membrane.

RNA Isolation and Quantitative Reverse Transcription-Polymerase Chain Reaction (qRT-PCR) Analysis

Total RNA was isolated from HUVECs using TRIzol reagent according to the manufacturer's protocol, and cDNA was obtained using the Transcriptor First Strand cDNA Synthesis Kit (Roche, Switzerland). Real-time PCR analysis was performed using Applied Biosystems SYBR Green Master Mix (Foster, CA, USA) in ABI Step One Plus Real-Time PCR system, GAPDH was used for normalization. **Supplementary Table 1** lists the PCR primer sequences.

Western Blot Analysis

Total protein was extracted using cell lysis buffer for Beyotime Western and Immunoprecipitation (Shanghai, China) following the manufacturer's instructions. Protein samples were separated by 10% sodium dodecyl sulfate–polyacrylamide gel electrophoresis and electroblotted to polyvinylidene difluoride membranes. The blots were blocked with 5% nonfat dry milk in Tris-buffered saline containing 0.1% Tween-20 (TBST), and then incubated overnight at 4℃ with appropriate primary antibodies. After TBST washing, membranes were incubated with a horseradish peroxidase-conjugated secondary

antibody diluted 1:5000 for 1 h at 18-25℃, and the blots were scanned and the intensity of the protein bands was quantified using Image-Pro Plus 6.0 software.

NF-kB Translocation

HUVECs were seeded onto glass coverslips at 1.0 $\times 10^5$ cells/well and grown to confluence. Coverslips were washed twice with PBS, fixed with 4% paraformaldehyde for 15 min at room temperature, and permeabilized with 0.4% Triton X-100 in PBS three times (10 min each). After incubation in blocking buffer (5% BSA in PBS) for 1 h, the permeabilized cells were incubated with 1:200 anti-NF-κB-p65 antibody overnight at 4℃. The coverslips were then washed with PBS and stained with Alexa Fluor 488 Anti-rabbit IgG (1:300) for 1 h at room temperature in the dark. Again, the coverslips were washed with PBS three times (10 min each), and cell nuclei were stained with 4′,6-diamidino-2-phenylindole for 5 min. Finally, coverslips were washed and fluorescent images were observed with a fluorescence microscope.

Statistical Analysis

Statistical analysis was conducted in SPSS 26.0 (IBM, USA). Continuous variables were expressed as mean ± SEM and categorical variables were expressed as the number and frequency of cases. Comparisons between the two groups were analyzed via unpaired Student's *t*-test for normally distributed variables or the chi-square test for categorical variables. Correlations between two continuous variables were expressed as Pearson's correlation coefficients. Multivariate analysis using a multiple linear regression model was performed to analyze the determinants of FGF23, and independent variables included age, gender, serum creatinine, serum calcium, and serum phosphorus. All *P*-values were two sided, and statistical significance was defined as $P<0.05$.

Results

Serum FGF23 was Associated with FMD Value in CAD Patients

FMD is a sensitive approach for endothelial and vascular function assessment. First, we used the FMD cutoff value of 2% to discriminate between the patients with severe endothelial dysfunction (FMD < 2%) from the remaining patients with nonsevere endothelial dysfunction (FMD ≥ 2%). **Table 1** presents the demographic, clinical, and laboratory features of the study population.

Compared with FMD ≥ 2% group, the smoker rate, levels of TG, DBP, LDL–C, ET-1, and phosphorus were higher, whereas the levels of HDL–C and NO level were lower in FMD <2% group ($P<0.05$). There were no statistical differences in age, gender, BMI, TC, FBG, SBP, creatinine, and calcium between the two groups ($P>0.05$).

It is noteworthy that compared with FMD ≥ 2% group, the levels of FGF23 were significantly increased in patients with FMD <2% [(786.43 ± 48.92) pg/mL vs. (469.45 ± 31.23) pg/mL] ($P<0.01$), which strongly indicated the role of FGF23 in endothelial dysfunction.

Serum FGF23 was Associated with Serum NO and ET-1 Levels in CAD Patients

Endothelial dysfunction is mainly caused by the change of these endothelium-derived relaxing and contracting mediators. To investigate the association of FGF23 with endothelial function, we further analyzed the correlation between FGF23 and endothelial function indicators, including NO and ET-1. In unadjusted analysis, FGF23 was positively correlated with serum Pi (r=0.472, $P<0.001$), serum creatinine (r=0.521, $P=0.006$), and ET-1 (r=0.369, $P=0.011$) and was negatively correlated with age (r=–0.256, $P=0.037$) and NO (r=–0.451, $P<0.001$). In multivariate-adjusted analysis, we further adjusted for age, gender, serum creatinine, serum calcium, and serum phosphorus; results showed that FGF23 was still associated with NO ($\beta=0.413$, $P=0.008$) and ET-1 ($\beta=-0.360$, $P=0.017$) **(Table 2)**.

These data suggested that high FGF23 serum levels were associated with endothelial dysfunction in CAD patients.

FGF23 Decreased NO Bioavailability and Induced ROS Production in HUVECs

To further determine if FGF23 interfered with the bioavailability of NO *in vitro*, we explored the effects of FGF23 on NO levels in HUVECs. For our experiments, we chose an exogenous FGF23 concentration of 10 ng/mL, which was based on the results of treatment with FGF23 in HUVECs at different concentrations and for different times **(Supplementary Fig. 1)**.

HUVECs were incubated with vehicle and FGF23 for 24 h; then, the cells were loaded with DAF-FM. Results showed that the fluorescence intensity of the FGF23 treated cells **(Fig. 1A-B)** was lower compared to the vehicle ($P<0.05$). Also, the concentration of nitrate was significantly reduced ($P<0.05$, **Fig. 1C**) in FGF23-stimulated HUVECs. However, western blotting demonstrated that FGF23 did not alter the phosphorylation Ser1177 and Thr495

Table 1. Characteristics of study population

Parameters	FMD ≥ 2% (n = 136)	FMD <2% (n = 185)	P-value
Age (years)	55.64 ± 11.33	52.06 ± 8.12	0.657
Male (%)	109 (58.91)	83 (61.02)	0.535
BMI (kg/m^2)	24.28 ± 2.76	20.39 ± 3.11	0.677
SBP (mmHg)	133.56 ± 15.76	126.32 ± 11.20	0.068
DBP (mmHg)	88.06 ± 15.37	96.45 ± 9.78	0.021
Coronary risk factors n (%)			
Hypertension	72 (52.94)	126 (68.10)	0.065
Dyslipidemia	98 (72.06)	142 (76.76)	0.716
Diabetes mellitus	45 (33.09)	65 (35.14)	0.625
Smoking	70 (37.84)	77 (56.62)	0.006
Family history of CAD	24 (17.64)	28 (15.14)	0.832
Medication use, n (%)			
Antihypertensive drugs	46 (33.82)	67 (36.22)	0.166
Lipid-lowering drugs	57 (41.91)	85 (45.95)	0.478
Antidiabetic drugs	15 (11.03)	22 (11.89)	0.751
Laboratory data			
FBG (mmol/L)	6.75 ± 0.86	7.18 ± 0.98	0.191
TC (mmol/L)	4.17 ± 0.83	4.56 ± 1.05	0.502
TG (mmol/L)	1.64 ± 0.54	1.95 ± 0.44	<0.001
HDL-C (mmol/L)	1.14 ± 0.14	0.87 ± 0.15	0.016
LDL-C (mmol/L)	2.28 ± 0.12	2.91 ± 0.15	<0.001
Scr (μmol/L)	84.24 ± 23.16	83.15 ± 28.54	0.558
Ca (mmol/L)	2.25 (2.16-2.38)	2.33 (2.25-2.37)	0.771
Pi (mmol/L)	1.55 ± 0.76	1.84 ± 0.49	0.011
NO (μmol/L)	41.84 ± 8.53	38.54 ± 7.66	0.023
ET-1 (pg/mL)	58.59 ± 5.63	67.35 ± 7.02	0.007
FGF23 (pg/mL)	469.45 ± 31.23	786.43 ± 48.92	<0.001

Data are mean ± SD unless indicated. BMI: body mass index; SBP: systolic blood pressure; DBP: diastolic blood pressure; FBG: fasting blood glucose; TC: total cholesterol; TG: triglyceride; HDL-C: high density lipoprotein cholesterol; LDL-C: low density lipoprotein cholesterol. Scr: Serum creatinine. Ca: Calcium. Pi: Phosphorus.

Table 2. Analysis of factors associated with FGF23

	Univariate analysis		Multiple linear regression analysis		
	Pearson's r	P-value	B(SE)	β	P-value
Age (years)	-0.256	0.037	-0.219 (0.122)	–0.274	0.088
Pi (mg/dL)	0.472	<0.001	0.351 (0.204)	0.309	0.099
Scr (mg/dL)	0.521	0.006	0.142 (0.366)	0.078	0.701
NO(μmol/L)	-0.451	<0.001	0.663 (0.230)	0.413	0.008
ET-1(pg/mL)	0.378	0.011	-0.287 (0.112)	-0.360	0.017

Pi: Serum phosphorus; Scr: Serum creatinine; B: regression coefficient; SE: standard deviation; β:standardized regression coefficient

site of eNOS (P>0.05, **Fig. 1D-E**).

Because the release of NO depends in part on the level of superoxide, we next explored the effects of FGF23 on ROS levels in HUVECs using DHE staining, cells treated with FGF23 had increased ROS levels (P<0.05, **Fig. 1F-G**) when compared with vehicle. Then, to confirm the ROS formation in HUVECs, we next detected the protein level of Nox2, p67phox, and p47phox in FGF23-treated cells. Results showed that FGF23 treatment significantly increased the expression of Nox2 **(Fig. 1H-I)**. Also, Nox2 cytosolic subunits p67phox and p47phox

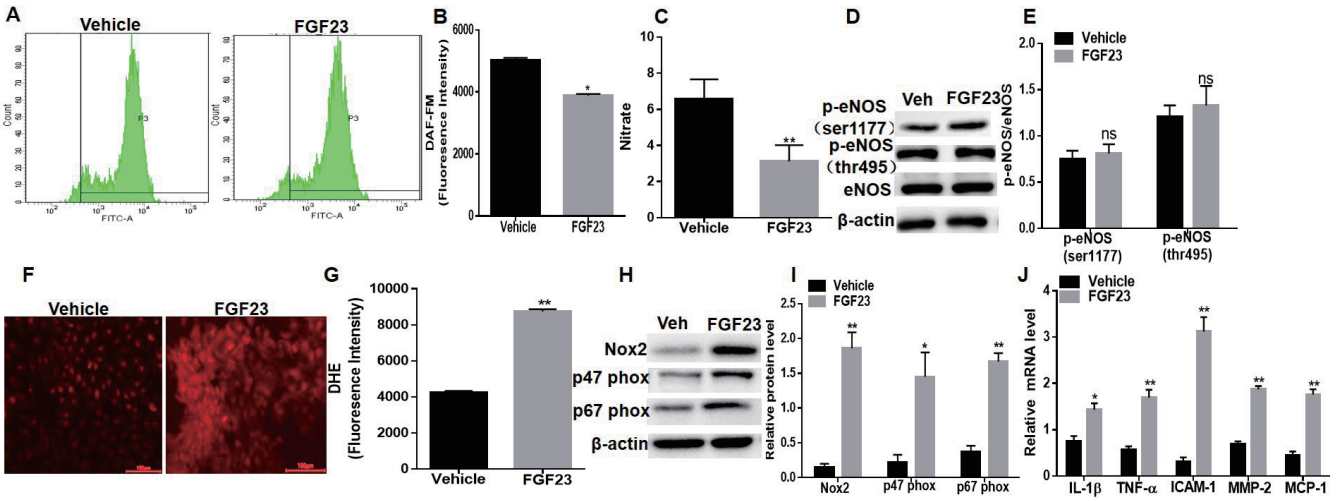

Fig. 1. Elevated FGF23 decreased NO bioavailability and induced ROS production in HUVECs

(A) HUVECs were incubated with vehicle and FGF23 for 24 h; then, the cells were loaded with DAF-FM, and the fluorescence intensity of the treated cells was detected by flow cytometry with the parameters of FITC. (B) Quantitative analysis of the relative DAF-FM fluorescence intensity. (C) The total nitrate was determined by the Griess reagent. (D and E) Protein levels of p-eNOS(ser1177) and p-eNOS(thr495) were determined via western blot analysis. D, Representative western blots. E, Relatively, results were quantified from the pixel values in grayscales ($n=3$). (F) HUVECs were incubated with vehicle and FGF23 for 24 h; then, the cells were loaded with DHE. Red fluorescence intensity was recorded using a fluorescence microscope. (G) Intensity of fluorescence was analyzed by Image-J software. (H and I) Protein levels of Nox2, p67phox, and p47phox were determined via western blot analysis. H, Representative western blots. I, Relatively, results were quantified from the pixel values in grayscales ($n=3$). (J) mRNA levels of IL-1, TNF-α, ICAM-1, MMP-2, and MCP-1 were detected via qRT-PCR. All values are shown as mean ± SEM; *$P<0.05$, **$P<0.01$ vs. vehicle.

necessary for Nox2 activation were stimulated by FGF23 treatment (Fig. 1H-I). These data indicate that FGF23 stimulated ROS production via activation of Nox2.

Subsequently, qRT-PCR results showed the mRNA levels of inflammatory cytokines IL-1 and TNF-α, intercellular adhesion molecule-1 (ICAM-1), matrix metalloproteinase-2 (MMP-2), and monocyte chemoattractant protein-1 (MCP-1) were significantly increased with FGF23 stimulation (Fig. 1J).

These data suggested that the bioavailability of NO was decreased in HUVECs potentially via the increased ROS production induced by FGF23.

FGF23 Promoted Cell Apoptosis and Attenuated Migration Ability in HUVECs

Then, to confirm the role of FGF23 in endothelial function, we further explored the effects of FGF23 on the cell activities of HUVECs. Western blot results showed that expression of apoptosis proteins, including Cleaved-Caspase3 and Bax, were significantly increased with FGF23 stimulation ($P<0.05$, Fig. 2A-B). Meanwhile, the ratio of apoptosis was greatly increased 1.6 times in HUVECs stimulated with FGF23 compared to the vehicle group ($P<0.05$, Fig. 2C-D). These data demonstrated the proapoptotic effect of FGF23 on HUVECs.

In addition, cell scratch assay and transwell cell migration assay were performed to evaluate the effects of FGF23 on migration characteristics of HUVECs. First, cell scratch test confirmed that the scratch wound healing rate of the FGF23 treatment was weaker than that of the vehicle group (1.86 ± 0.02 vs 8.98 ± 0.87, $P<0.01$, Fig. 2E-F), whereas transwell assay also reported that FGF23 treatment impaired the cell migratory ability, which was evidenced by a decreased number of transmembrane migrating cells by 62.86% (96.33 ± 10.20 vs 37.67 ± 9.13, $P<0.05$, Fig. 2G-H).

Taken together, these data confirmed that FGF23 led to endothelial dysfunction by promoting HUVECs apoptosis and attenuating the migration of HUVECs.

FGF23 activated the NF-κB signaling pathway in HUVECs

To shed light on the signaling pathway induced by FGF23, we next detected the protein levels of the key members of NF-κB signaling pathways by western blot analysis. Western blots showed increased protein level of cytosolic p-p65/p65, p-IκBα, and decreased protein level of IκBα with FGF23 stimulation ($P<0.05$, Fig. 3A-B). Furthermore, we detected the NF-κB activation using immunofluorescent analysis.

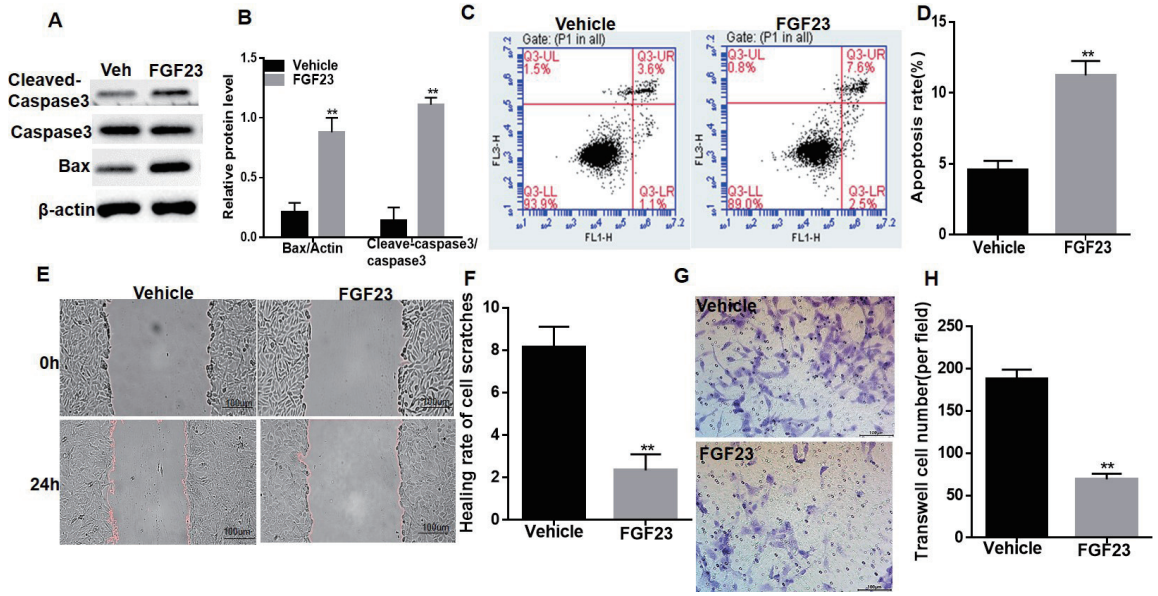

Fig. 2. Elevated FGF23 promoted cell apoptosis and attenuated cell migration ability in HUVECs

(A and B) Protein levels of Caspase3, Cleaved-Caspase3, and Bax were detected via western blot analysis. A, Representative western blots. B, Relatively, results were quantified from the pixel values in grayscales ($n=3$). (C and D) Apoptosis of HUVECs was measured via annexin-V-conjugated Flow Cytometry analysis. The apoptosis rate of HUVECs treated with vehicle and FGF23 was quantitatively analyzed ($n=3$). (E) Representative results of scratches on HUVECs cells treated with vehicle and FGF23. (F) Quantitative analysis of healing rate of scratch area ($n=5$). (G) Representative results of transwell cell migration in HUVECs after treatment with vehicle and FGF23. (H) Quantitative analysis of mean cell count per field on the transwell compartment membrane after treatment with vehicle and FGF23. All data are represented as the mean ± SEM of at least three independent experiments. $^{*}P<0.05$, $^{**}P<0.01$ vs. vehicle.

Results showed that p65 NF-κB translocation was significantly activated with FGF23 treatment in HUVECs **(Fig. 3C)**.

Furthermore, we found in our previous experiments that FGFR expression was elevated in aortas of AS mice and FGF23-stimulated HUVECs **(Supplementary Fig. 2)**, and the previous report confirmed the direct effect of FGF23 in endothelium by activating FGF receptor[7]. Thus, for the further experiment, HUVECs were incubated with the NF-κB inhibitor BAY11-7082 (10 μM) or FGFR antagonist BGJ398 (2 μM) for 30 min before treatment with FGF23, we found that preincubation with BAY11-7082 or BGJ398 could effectively prevent the endothelium injury caused by FGF23, expression of Cleaved-Caspase3 and Bax was significantly decreased compared with FGF23 stimulation alone ($P<0.05$, **Fig. 3D-E**). The apoptosis of HUVECs by FGF23 is inhibited by the BAY11-7082 **(Supplementary Fig. 3A-B)**; otherwise, the decreased healing rate of scratch area and decreased transwell cell migration by FGF23 was improved by BAY11-7082 **(Supplementary Fig. 3)**.

Based on these results, we concluded that FGF23 contributed to endothelial dysfunction through the activation of the NF-κB signaling pathway.

Discussion

Numerous reports have identified an association between elevated FGF23 levels and cardiovascular events[12, 13]. Nevertheless, the results of the existing studies remain controversial. For example, the Prospective Investigation of the Vasculature in Uppsala Seniors (PIVUS) study revealed that FGF23 was associated with vascular dysfunction in the community[14], but a 10 year follow-up study did not find a relationship between FGF23 level and the development of incident CAD in men without chronic kidney disease[15], more research is still needed to reveal the role and mechanism of FGF23 in CAD. In the present study, we demonstrated for the first time the correlation between FGF23 and endothelial dysfunction on the basis of the clinical data of patients with CAD and functional research in HUVECs. Our data suggest that in states of Klotho deficiency, e.g. CAD, elevated FGF23 triggers the generation of ROS by activating NADPH oxidase. Increased ROS induces NF-κB p65 phosphorylation, subsequently triggering nuclear translocation of NF-κB p65 to

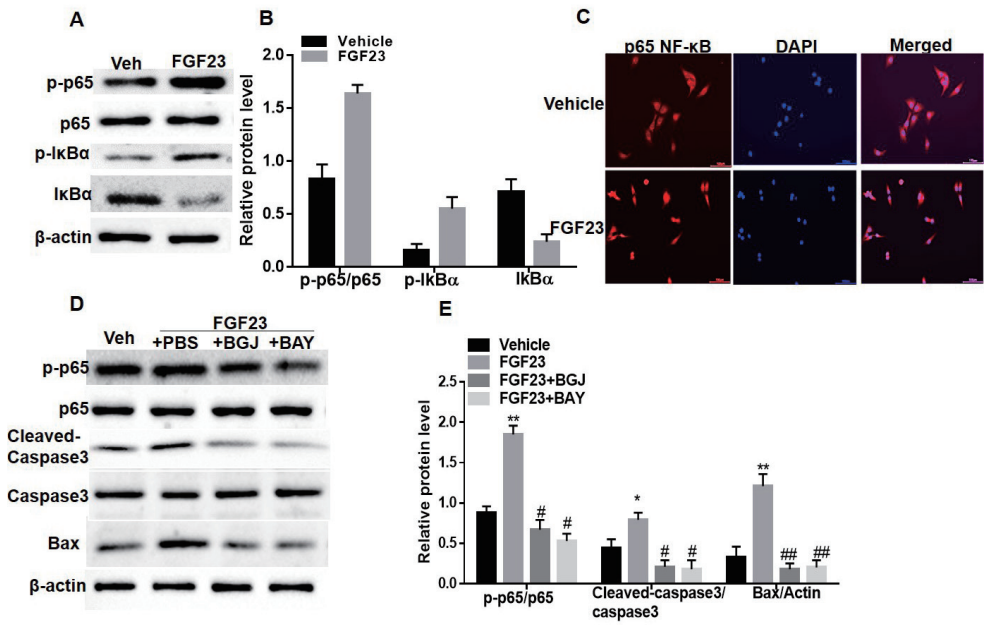

Fig. 3. Elevated FGF23 activated the NF-κB signaling pathway in HUVECs

(A) Western blot analysis revealed representative results of p-p65, p65,p-IκBα, and IκBα protein expression after FGF23 treatment. (B) Quantitative analysis of the ratio of p-p65 to p65, p-IκBα, and IκBα to β-actin after FGF23 treatment ($n=3$). (C) Immunofluorescence detection of P65 NF-κB translocation in HUVECs after treatment with FGF23 (magnified, ×100, scale=100 μm). (D) HUVECs were incubated with the NF-κB inhibitor BAY11-7082 (10 μM) or FGFR antagonist BGJ398 (2 μM) for 30 min before treatment with FGF23, protein levels of p-p65 to p65, Cleaved-Caspase3, and Bax were determined via western blot analysis. (E) Results were quantified from the pixel values in grayscales ($n=3$). All experiments were repeated three times. $^{*}P<0.05$, $^{**}P<0.01$ vs. vehicle. $^{\#}P<0.05$, $^{\#\#}P<0.01$ vs. FGF23 treatment.

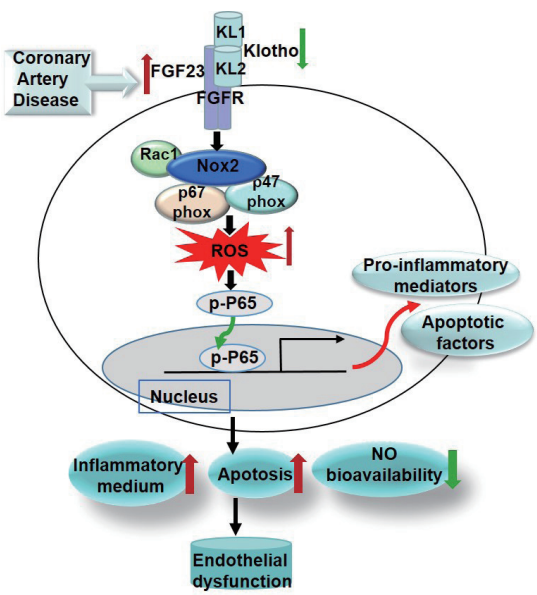

Fig. 4. Schematic representation of the mechanisms underlying the association between FGF23 and endothelial function

express proinflammatory mediators and apoptotic factors, thus reducing NO bioavailability, increasing the apoptosis of HUVECs, and consequently leading to endothelial dysfunction (**Fig. 4**).

FMD is currently the most widely used noninvasive method to detect vascular endothelial function[16]. FMD of the damaged humeral artery is an indicator of endothelial function injury and is

associated with future cardiovascular events in patients with CAD[17]. In this study, subjects were first divided into two groups according to the FMD values; we used the FMD cutoff value of 2% to discriminate patients with severe endothelial dysfunction from the remaining patients with nonsevere endothelial dysfunction. Results showed that serum FGF23 levels were significantly increased in patients with severe endothelial dysfunction, which strongly suggested the role and impact of FGF23 in endothelial dysfunction.

Additionally, endothelial dysfunction is mainly caused by reduced production or action of the relaxing mediators, the best characterized endothelium-derived relaxing factor is NO, and the release of ET-1 contributes to endothelial dysfunction[18]. Results in the present study showed that FGF23 was negatively correlated with NO level but was positively correlated with ET-1 level, independent of confounders such as age, gender, serum creatinine, serum calcium, and serum phosphorus. These data further revealed the correlation between FGF23 and endothelial function. Furthermore, we confirmed the association of FGF23 with endothelial dysfunction through further *in vitro* research in HUVECs. FGF23 interfered with the bioavailability of NO in HUVECs, thereby mediating endothelial injury, as characterized by promoting HUVECs apoptosis and attenuating the migration of HUVECs. All these findings from *in vitro* studies were fundamentally consistent with the view of the clinical data in CAD patients.

Some reports previously revealed the direct or indirect effect of FGF23 on endothelium[7]. In our previous experiments, we constructed the AS model of ApoE-knockout mouse fed on a high-fat diet, serum FGF23 was elevated in the AS mice, and the protein level of *Fgfr1* was significantly increased in the aortas of the AS mice **(Supplementary Fig. 2)**. Moreover, recently, an association of high FGF23 serum levels with impaired endothelium-dependent vasodilatation was proved in *Col4a3*$^{-/-}$ mice. The *Col4a3*$^{-/-}$ mouse is an animal model of human autosomal-recessive Alport syndrome, showing Chronic kidney disease (CKD) and high FGF23 serum levels compared with wild-type littermates. Results in the *Col4a3*$^{-/-}$ mice model suggested that high FGF23 serum levels cause endothelial dysfunction by decreasing NO bioavailability and increasing superoxide[8]. Moreover, another report provided evidence that FGF23 was a cause of peripheral endothelial dysfunction in a model of early CKD and that endothelial dysfunction in CKD can be prevented by blocking FGF23[19]. In line with these findings, the present study showed a positive association between high FGF23 serum concentrations and vascular dysfunction. Data in the present study showed that FGF23 did not alter the phosphorylation Ser1177 and Thr495 site of eNOS. Contrary to our findings, a recent study investigated that FGF23 could activate eNOS phosphorylation in HCAEC[10]. Conflicting observations may result from the type of vessel and endothelial cells and different states of Klotho; they stimulated cells with FGF23 for 15 and 30 min and focused on the acute effects of FGF23. Moreover, existing evidence[8, 10] has shown that in states of Klotho deficiency, FGF23-mediated NO synthesis was blunted and ROS formation overruled ROS degradation. Objects of the present study were patients with CAD, these patients are in a state of Klotho deficiency[20]. Furthermore, in HUVECs, we chose an FGF23 concentration of 10 ng/mL for 24 h, which resembled those found in moderate stages of CKD, for example, ~300-fold increase of FGF23 compared with healthy subjects[21], so the results of this study represented the correlation of FGF23 and endothelial function in a state of Klotho deficiency.

Finally, it is worth noting in the present study that NF-κB signaling in HUVECs is activated by FGF23. NF-κB is a protein formed by a dimeric transcription factor family, which regulates the expression of inflammatory factors and apoptosis or survival of cells[22]. We supported a novel hypothesis that activation of the NF-κB pathway may be one of the key mechanisms underlying the effect of FGF23 in endothelial injuries.

The present study does have some limitations. This was an observational study with a relatively small population size, and further prospective studies are warranted to confirm the relationship between FGF23 and endothelial dysfunction in a larger population. Additionally, future functional *in vivo* studies in different mouse models of FGF23 excess will be needed to pursue the interaction between FGF23 and endothelial dysfunction.

Conclusion

In summary, this study confirmed that elevated FGF23 led to endothelial dysfunction through the activation of the NF-κB signaling pathway. Hence, this study lays a solid foundation for further studies aimed at identifying a potential therapeutic target for endothelial dysfunction based on FGF23 and its related receptors.

Acknowledgment

This work is supported by the National Natural Science Fund Program of China (No.81900391) and

the Key Scientific Research Project of Henan Province (No.22A310006).

Conflicts of Interest

The manuscript has been read and approved by all authors for publication and all authors declare no conflicts of interest.

References

1) Rajendran P, Rengarajan T, Thangavel J, Nishigaki Y, Sakthisekaran D, Sethi G, Nishigaki I: The vascular endothelium and human diseases. Int J Biol Sci, 2013; 9: 1057-1069
2) Godo S, Shimokawa H: Endothelial functions. Arterioscler Thromb Vasc Biol, 2017; 37: e108-e114
3) Gohil A, Imel EA: FGF23 and associated disorders of phosphate wasting. Pediatr Endocrinol Rev, 2019; 17: 17-34
4) Rodríguez M: FGF23: Is it another biomarker for Phosphate-Calcium metabolism? Adv Ther, 2020; 37: 73-79
5) Lu X, Hu MC: Klotho/FGF23 axis in chronic kidney disease and cardiovascular disease. Kidney Dis (Basel), 2017; 3: 15-23
6) Chou F, Chen J, Huang S, Chan Y, Chi S, Chen W: Changes in serum FGF23 and Klotho levels and calcification scores of the abdominal aorta after parathyroidectomy for secondary hyperparathyroidism. Am J Surg, 2019; 218: 609-612
7) Six I, Okazaki H, Gross P, Cagnard J, Boudot C, Maizel J, Drueke T B, Massy ZA: Direct, acute effects of Klotho and FGF23 on vascular smooth muscle and endothelium. PLoS One, 2014; 9: e93423
8) Silswal N, Touchberry CD, Daniel DR, McCarthy DL, Zhang S, Andresen J, Stubbs JR, Wacker MJ: FGF23 directly impairs endothelium-dependent vasorelaxation by increasing superoxide levels and reducing nitric oxide bioavailability. Am J Physiol Endocrinol Metab, 2014; 307: E426-436
9) Lindberg K, Olauson H, Amin R, Ponnusamy A, Goetz R, Taylor RF, Mohammadi M, Canfield A, Kublickiene K, Larsson TE: Arterial Klotho expression and FGF23 effects on vascular calcification and function. PLoS One, 2013; 8: e60658
10) Richter B, Haller J, Haffner D, Leifheit-Nestler M: Klotho modulates FGF23-mediated NO synthesis and oxidative stress in human coronary artery endothelial cells. Pflugers Arch, 2016; 468: 1621-1635
11) Corretti MC, Anderson TJ, Benjamin EJ, Celermajer D, Charbonneau F, Creager MA, Deanfield J, Drexler H, Gerhard-Herman M, Herrington D, Vallance P, Vita J, Vogel R: Guidelines for the ultrasound assessment of endothelial dependent flow mediated vosodilation of the brachial artery: a report of the International Brachial Artery Reactivity Task Force. J Am Coll Cardiol, 2002; 39: 2572265
12) Jimbo R, Shimosawa T: Cardiovascular risk factors and chronic kidney disease-FGF23: a key molecule in the cardiovascular disease. Int J Hypertens, 2014; 2014: 381082
13) Marthi A, Donovan K, Haynes R, Wheeler DC, Baigent C, Rooney CM, Landray MJ, Moe SM, Yang J, Holland L, Giuseppe R, Krijger AB, Mihaylova B, Herrington WG: Fibroblast Growth Factor-23 and Risks of Cardiovascular and Noncardiovascular Diseases: A Meta-Analysis. J Am Soc Nephrol, 2018; 29: 2015-2027
14) Mirza M AI, Larsson A, Lind L, Larsson TE: Circulating fibroblast growth factor-23 is associated with vascular dysfunction in the community. Atherosclerosis, 2009; 205: 385-390
15) Taylor EN, Rimm EB, Stampfer MJ, Curhan GC: Plasma fibroblast growth factor 23, parathyroid hormone, phosphorus, and risk of coronary heart disease. Am Heart J, 2011; 161: 956-962
16) Soares RN, Somani YB, Proctor DN, Murias JM: The association between near-infrared spectroscopy-derived and flow-mediated dilation assessment of vascular responsiveness in the arm. Microvasc Res, 2019; 122: 41-44
17) Tremblay JC, Pyke KE: Flow-mediated dilation stimulated by sustained increases in shear stress: a useful tool for assessing endothelial function in humans? Am J Physiol Heart Circ Physiol, 2018; 314: H508-H520
18) Roumeliotis S, Mallamaci F, Zoccali C: Endothelial Dysfunction in Chronic Kidney Disease, from Biology to Clinical Outcomes: A 2020 Update. J Clin Med, 2020; 9: 2359
19) Verkaik M, Juni RP, van Loon E PM, van Poelgeest EM, Kwekkeboom Rick F J, Gam Z, Richards WG, Wee P M Ter, Hoenderop JG, Eringa EC, Vervloet MG: FGF23 impairs peripheral microvascular function in renal failure. Am J Physiol Heart Circ Physiol, 2018; 315: H1414-H1424
20) Sarmento-Dias M, Santos-Araújo C, Poínhos R, Oliveira B, Silva IS, Silva LS, Sousa MJ, Correia F, Pestana M: Fibroblast growth factor 23 is associated with left ventricular hypertrophy, not with uremic vasculopathy in peritoneal dialysis patients. Clin Nephrol, 2016; 85: 135-141
21) D'Arrigo G, Pizzini P, Cutrupi S, Tripepi R, Tripepi G, Mallamaci F, Zoccali C: FGF23 and the PTH response to paricalcitol in chronic kidney disease. Eur J Clin Invest, 2020; 50: e13196
22) Karunakaran D, Nguyen MA, Geoffrion M, Vreeken D, Lister Z, Cheng HS, Otte N, Essebier P, Wyatt H, Kandiah JW, Jung R, Alenghat FJ, Mompeon A, Lee R, Pan C, Gordon E, Rasheed A, Lusis AJ, Liu P, Matic LP, Hedin U, Fish JE, Guo L, Kolodgie F, Virmani R, van Gils JM, Rayner KJ: RIPK1 Expression Associates With Inflammation in Early Atherosclerosis in Humans and Can Be Therapeutically Silenced to Reduce NF-kappaB Activation and Atherogenesis in Mice. Circulation, 2021; 143: 163-177

Supplemental Table 1. DNA sequence of all real-time PCR primers

Primer Name	Sequence (5'-3')	Products(bp)
IL1B-F	GCCAGTGAAATGATGGCTTATT	85
IL1B-R	AGGAGCACTTCATCTGTTTAGG	
TNFA-F	AAGGACACCATGAGCACTGAAAGC	125
TNFA-R	AGGAAGGAGAAGAGGCTGAGGAAC	
ICAM1-F	TGCAAGAAGATAGCCAACCAAT	80
ICAM1-R	GTACACGGTGAGGAAGGTTTTA	
MMP2-F	ATTGTATTTGATGGCATCGCTC	202
MMP2-R	ATTCATTCCCTGCAAAGAACAC	
MCP1-F	AGAATCACCAGCAGCAAGTGTCC	98
MCP1-R	TCCTGAACCCACTTCTGCTTGG	
GAPDH-F	AGCCACATCGCTCAGACAC	135
GAPDH-R	GCCCAATACGACCAAATCC	

F, forward; R, reverse.

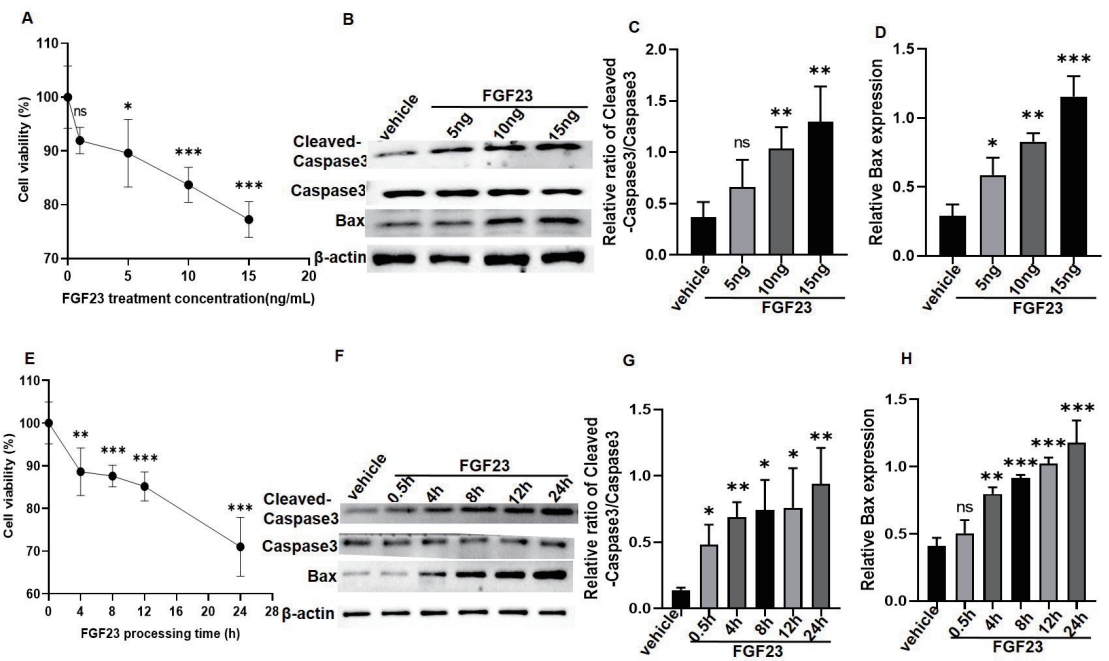

Supplementary Fig. 1. Treatment with FGF23 in HUVECs at different concentrations and for different times

(A) Relative numbers of HUVECs after FGF23 treatment at different concentrations were calculated by CCK-8 assay ($n=5$). (B to D) Western blotting assay detected representative results of Caspase3 and cleaved-caspase3 protein expression in HUVECs after FGF23 treatment at 0,5,10 and 15ng/mL. (E) Relative numbers of HUVECs after FGF23 treatment for different times were calculated by CCK-8 assay ($n=5$) (F to H) Western blotting assay detected representative results of Caspase3 and cleaved-caspase3 protein expression in HUVECs at 0, 0.5, 4, 8, 12, and 24 h after 10ng/mL FGF23 treatment. (D) Quantitative analysis of the ratio of Cleaved-Caspase to Caspase3 at 0, 0.5, 4, 8, 12, and 24 h after 10ng/mL FGF23 treatment. All values are shown as mean ± SEM; *$P<0.05$, **$P<0.01$, ***$P<0.001$ vs. vehicle.

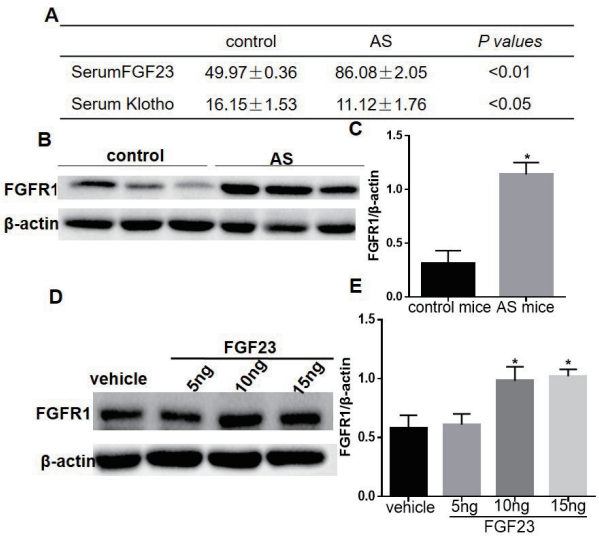

Supplementary Fig. 2. Serum FGF23 in AS mice and Expression of FGFR in aortas of AS mice and in FGF23-stimulated HUVECs

(A) Levels of serum FGF23 and klotho were detected by the ELISA method. Control mice, $n=10$; AS mice, $n=10$; (B and C) Protein levels of FGFR1 in aortas of AS mice were determined by Western blot analysis. B, representative Western blots. C, results were quantified from the pixel values in grayscales. Control mice, $n=10$; AS mice, $n=10$; (D and E) Protein levels of FGFR1 in FGF23-stimulated HUVECs were determined by Western blot analysis. D, representative Western blots. E, results were quantified from the pixel values in grayscales ($n=3$). $^{*}P<0.05$, $^{**}P<0.01$ vs. control mice or vehicle.

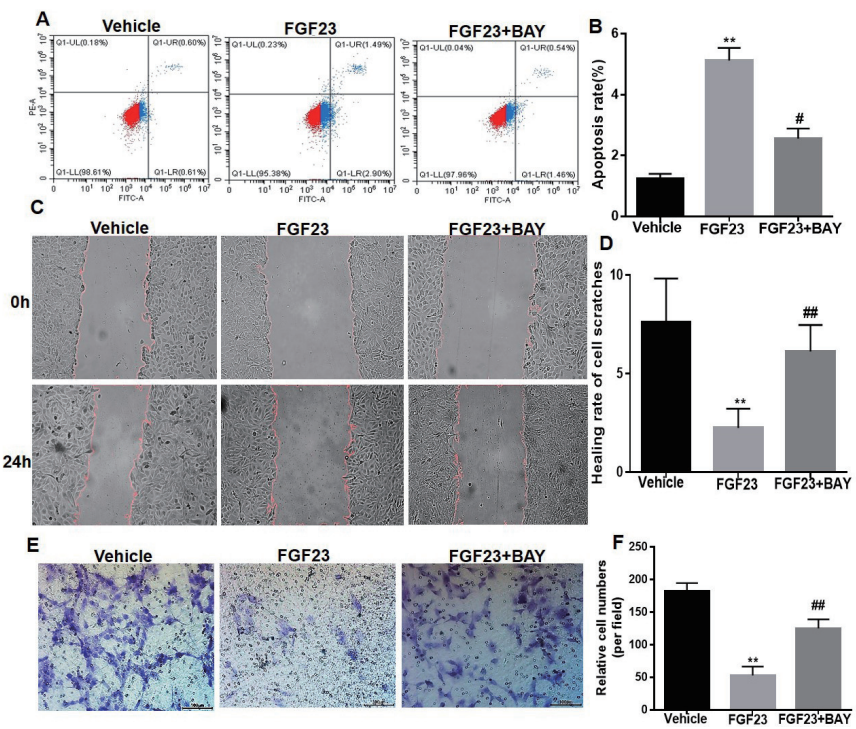

Supplementary Fig. 3. Preincubation with BAY11-7082 prevents the endothelium injury caused by FGF23

(A) HUVECs were incubated with the NF-κB inhibitor BAY11-7082 (10 uM) for 30 min before treatment with FGF23. Apoptosis of HUVECs was measured via Annexin-V conjugated FACS analysis. (B)The apoptosis rate of HUVECs pretreated with or without BAY11-7082 was quantitatively analyzed ($n=3$). (C) Representative results of scratches on HUVECs cells pretreated with or without BAY11-7082. (D)Quantitative analysis of healing rate of scratch area ($n=5$). (E) Representative results of Transwell cell migration in HUVECs after pretreatment with or without BAY11-7082. (F)Quantitative analysis of mean cell count per field on the Transwell compartment membrane after pretreatment with or without BAY11-7082. All data are represented as the mean±SEM of at least three independent experiments. $^{*}P<0.05$, $^{**}P<0.01$ vs. vehicle. $^{\#}P<0.05$, $^{\#\#}P<0.01$ vs. DMSO.